Nanoindentation and Tribological Performance of Magnetron Sputtered FeCrCoMnNi High-Entropy Alloy Coatings

***Matej Kljajo*[1], *Ivan Peko*[2], *Nikša Čatipović*[3] *and Anatoliy Zavdoveev*[4]**

1) University of Mostar, Faculty of Mechanical Engineering, Computing and Electrical Engineering, Matice hrvatske bb, 88000 Mostar, Bosnia and Herzegovina

2) University of Split, Faculty of Science, Ruđera Boškovića 33, 21000 Split, Croatia

3) University of Split, Faculty of Electrical Engineering, Mechanical Engineering and Naval Architecture, Ruđera Boškovića 32, 21000 Split, Croatia

4) Paton Electric Welding Institute of NAS of Ukraine, K.Malevicha 11, 03150 Kiev, Ukraine

Corresponding author: matej.kljajo@fsre.sum.ba

Type of paper: Original Scientific Paper

Abstract: High-entropy alloy (HEA) coatings have attracted considerable attention due to their promising mechanical and tribological properties. In this study, a FeCrCoMnNi HEA target fabricated by the Wire Arc Additive Manufacturing (WAAM) process was used for the deposition of coatings on SS316L stainless steel substrates by DC magnetron sputtering under different deposition conditions by varying the argon flow rate (10–20 sccm), sputtering power (100–200 W), and deposition time (20–40 min). The tribological behavior of the coatings was evaluated using an Anton Paar TRB3 tribometer under dry sliding ball-on-disc conditions with a ruby counter-body, while nanoindentation measurements were performed with HIT3 nanoindentor to determine the hardness and elastic modulus of the coatings. The coated samples exhibited improved mechanical properties compared to the uncoated substrate, confirming the strengthening effect of the deposited HEA layers.

Keywords: *Coatings; Magnetron Sputtering; High Entropy Alloys; Tribological properties, Nanoindentation*

1. Introduction

High-entropy alloy (HEA) coatings or High Entropy Coatings (HEC) have emerged as a promising class of advanced surface materials due to their unique multi-element composition and attractive combination of mechanical and tribological properties [1], [2], [3]. Owing to their high hardness [4], thermal stability [5], [6], and resistance to wear and corrosion [7], [8], [9], [10], HEA coatings are increasingly considered for applications exposed to demanding operating conditions, including aerospace, marine, and energy systems. Among the various fabrication techniques, magnetron sputtering has proven to be a highly versatile method for producing HEA coatings with controlled chemical composition, dense microstructure, and good coating uniformity [4], [11], [12], [13].

The properties and performance of magnetron sputtered coatings are strongly influenced by deposition parameters such as sputtering power, working gas flow, and deposition time, since these parameters directly affect plasma characteristics, atom transport, coating growth, and phase evolution [14]. Consequently, optimization of the deposition process plays a crucial role in achieving desirable tribological behavior and surface stability. Recent studies have demonstrated that variations in sputtering conditions can significantly modify the friction response, microstructure, and overall performance of various types of coatings and thin films [15], [16], [17], [18], [19]. Understanding the tribological behavior and surface properties of thin films and coatings is essential for their effective implementation in demanding engineering applications, including aerospace, marine, and energy systems. Previous studies [20], [21] have emphasized that friction behavior strongly influences both energy efficiency and wear performance in mechanical components.

In this context, the present study investigates the tribological behavior of FeCrCoMnNi HEA coatings deposited on SS316L stainless steel substrates by DC magnetron sputtering using a WAAM-fabricated HEA target. Special attention is focused on the influence of deposition parameters on the friction behavior and hardness of the obtained coatings.

2. Materials and methods

The FeCrCoMnNi high-entropy alloy (HEA) target employed for coating deposition was fabricated using the Wire Arc Additive Manufacturing (WAAM) process at the Paton Electric Welding Institute in Kiev, Ukraine. Following fabrication, the deposited material was machined into a disc-shaped target with a diameter of 3 inches and a thickness of 6 mm, as shown in Figure 1. Both target surfaces were subsequently ground and polished to ensure adequate contact with the target holder within the vacuum chamber during the deposition process. The chemical composition is shown in Figure 2.

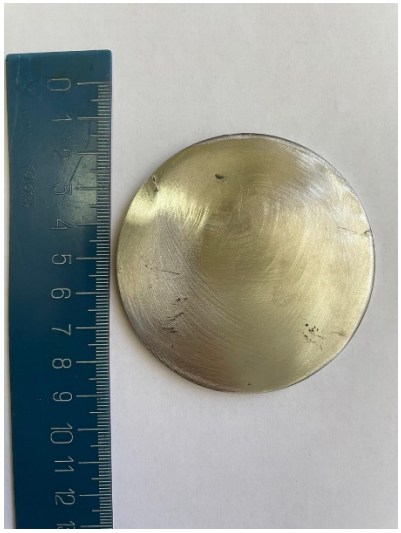
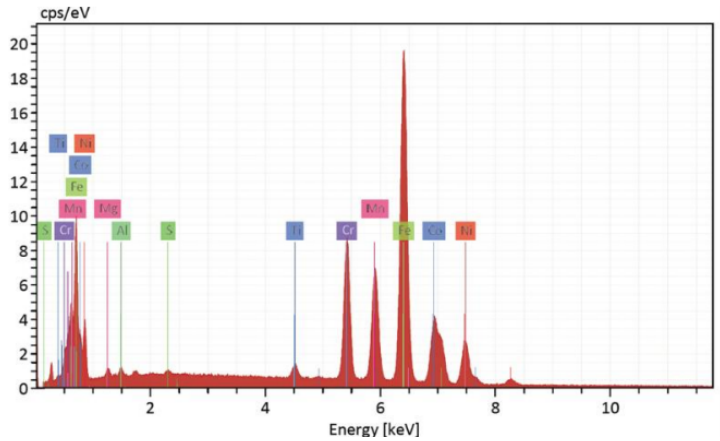


Figure 1. *Chemical High Entropy Alloy target*



Acquisition

Element	At. No.	Netto	Mass [%]	Mass Norm. [%]	Atom [%]
Magnesium	12	2115	0.44	0.41	0.92
Aluminium	13	1016	0.16	0.15	0.30
Sulfur	16	1009	0.12	0.11	0.19
Titanium	22	7012	1.06	0.98	1.13
Chromium	24	82591	14.00	12.95	13.77
Manganese	25	61587	13.19	12.20	12.28
Iron	26	206739	55.27	51.12	50.63
Cobalt	27	38213	12.88	11.91	11.18
Nickel	28	28555	11.02	10.19	9.60
		Sum	**108.13**	**100.00**	**100.00**

Figure 2. *Chemical composition of High Entropy Alloy Target*

The obtained HEA target was subsequently employed for the deposition of thin films onto stainless steel substrates by DC magnetron sputtering. Coated samples are shown in Figure 3. Prior to the deposition process, the substrates were mechanically prepared and cleaned to ensure adequate surface quality and proper coating adhesion. The surface preparation procedure included sequential grinding and polishing to a mirror-like finish, followed by ultrasonic cleaning and degreasing in acetone to remove residual contaminants and surface impurities from the substrate surface. Coating deposition was performed using a DC magnetron sputtering system and chamber VacuumPffeifer 250,

as shown in Figure 4. Prior to deposition, the sputtering chamber was evacuated to the base pressure of 2.1×10^{-5} mbar, after which argon was introduced as the working gas. The deposition process was carried out under different sputtering conditions by varying the sputtering power, argon flow rate, and deposition time as shown in Table 1, to investigate their influence on the tribological behaviour and hardness of the coatings.



Figure 3. *Coated Samples*



Figure 4. *Magnetron sputtering vacuum chamber Pfeiffer Vacuum Classic 250*

The investigated deposition parameters are presented in Table 1.

Table 1. *Experiment plan – deposition parameters for the 9 coated specimens.*

No	Argon flow [sccm]	Power [W]	Time [min]
1	10	100	20
2	10	150	30
3	10	200	40
4	15	100	30
5	15	150	40
6	15	200	20
7	20	100	40
8	20	150	20
9	20	200	30

The tribological behaviour of the deposited HEA coatings was evaluated using a tribometer Anton Paar TRB3 employing the ball-on-disc testing configuration under dry sliding conditions, as shown on Figure 5. A ruby ball 6 mm in diameter was used as the counter-body material. Tribological tests were

performed under different operating conditions to evaluate the influence of sliding parameters on the friction behaviour of the coatings. The experiments were conducted at room temperature using different combinations of normal load, sliding radius, and rotational speed. The applied testing conditions are summarized in Table 2.

The coefficient of friction (COF) was continuously recorded during testing, and the obtained results were analysed using the average friction coefficient and standard deviation values to evaluate the stability of the tribological response of the investigated coatings. In addition, the evolution of the friction coefficient throughout the test duration was monitored to identify possible running-in effects and changes in the wear mechanism during sliding. The obtained tribological data were subsequently correlated with the mechanical properties of the coatings to provide a comprehensive evaluation of their performance.

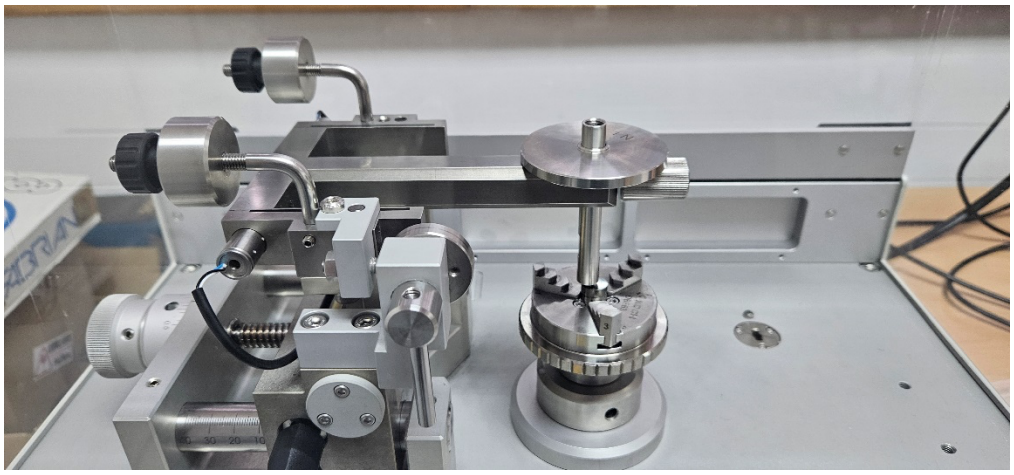


Figure 5. *Experimental setup of the TRB3 tribometer used for tribological testing.*

Table 2. *Operating Conditions for the tribological testing*

	Test 1	Test 2	Test 3	Test 4
Sliding radius [mm]	2	3	4	5
Load [N]	1	1	2	2
Rotational speed [rpm]	5	10	5	10

The mechanical properties of the deposited coatings were further investigated by nanoindentation testing using an Anton Paar HIT3 nanoindenter, as shown in Figure 6. Measurements were performed with a Berkovich diamond indenter at maximum loads of 5, 10, and 15 mN, while the detailed testing conditions are presented in Table 3.



Figure 6. *Experimental setup for nanoindentation measurements using the Anton Paar HIT3 nanoindenter*

For each sample and each loading condition, three individual indents were performed at different, spatially separated locations on the specimen surface in order to ensure statistical relevance and to account for possible local heterogeneities. The obtained load–displacement data were subsequently used for the determination of hardness (HVIT/HIT) and reduced elastic modulus (E*), using the Oliver and Phaar method.
As a representative value for each sample and load level, the arithmetic mean of the three measurements was calculated and taken as the final reported result. This approach provides a more reliable and reproducible estimation of the mechanical response by minimizing the influence of local surface irregularities or experimental scatter.

Table 3. *Operating Conditions for the nanoindentation testing*

	Test 1	Test 2	Test 3
Force [mN]	5	10	15
Loading rate [mN/min]	10	20	10
Unloading rate [mN/min]	10	20	30
Pause [s]	10	10	30
Acquisition rate [Hz]	10	10	10

3. Results and Discussion

3.1. Tribological measurements

Table 4 presents the average coefficient of friction (COF) values and corresponding standard deviations obtained for all investigated HEA coatings under different sliding conditions. The tribological measurements revealed noticeable differences in friction behaviour among the investigated samples, indicating a significant influence of the deposition parameters on the tribological response of the coatings. The sample designated SS316 represents the uncoated stainless steel sample, while 1-9 correspond to samples with varied sputtering parameters, as listed in Table 1.

Table 4. *Coefficient of friction measurement results*

	Test 1		Test 2		Test 3		Test 4	
	μ	± Std Dev	μ	± Std Dev	μ	± Std Dev	μ	± Std Dev
1	0,261	0,048	0,296	0,051	0,262	0,052	0,509	0,268
2	0,580	0,181	0,669	0,147	0,582	0,237	0,574	0,315
3	0,593	0,170	0,564	0,166	0,592	0,227	0,623	0,297
4	0,423	0,245	0,390	0,152	0,426	0,272	0,328	0,222
5	0,734	0,132	0,807	0,102	0,736	0,223	0,858	0,270
6	0,504	0,172	0,527	0,184	0,510	0,220	0,413	0,215
7	0,623	0,160	0,683	0,185	0,627	0,209	0,626	0,264
8	0,571	0,163	0,539	0,176	0,572	0,215	0,520	0,244
9	0,583	0,200	0,506	0,175	0,589	0,251	0,548	0,264
SS316	0,256	0,050	0,215	0,027	0,258	0,055	0,170	0,030

In general, increasing the sliding severity, particularly at higher sliding radius and load, resulted in higher COF values and larger friction fluctuations. This trend was especially evident during the Test 4 (5 mm / 2 N / 10 rpm), where most samples exhibited increased average friction coefficients and higher standard deviation values compared to less severe testing conditions. The increase in standard deviation suggests a less stable sliding contact and more pronounced friction fluctuations under aggressive operating conditions

Among the investigated coatings, sample 4 demonstrated the most favorable tribological behaviour under the most severe testing conditions, exhibiting the lowest average COF value (μ = 0.328) among all coated samples during the Test no 4, as illustrated in Figure 7.

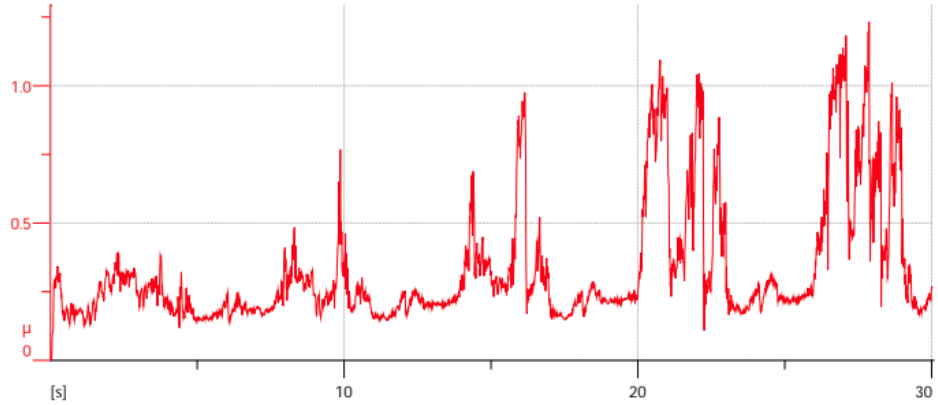


Figure 7. *Tribological measurement on sample 4 in test 4*

In contrast, sample 5 consistently showed the highest friction coefficients in all testing regimes, indicating a less favourable tribological response and increased friction during sliding.
The obtained results also showed that several coatings maintained relatively stable friction behaviour despite variations in testing conditions, which may indicate good coating homogeneity and stable contact conditions during sliding.
Overall, the results confirm that the tribological behaviour of FeCrCoMnNi HEA coatings deposited by DC magnetron sputtering strongly depends on both the deposition parameters and the applied sliding conditions.

3.2. Nanoindentation measurements

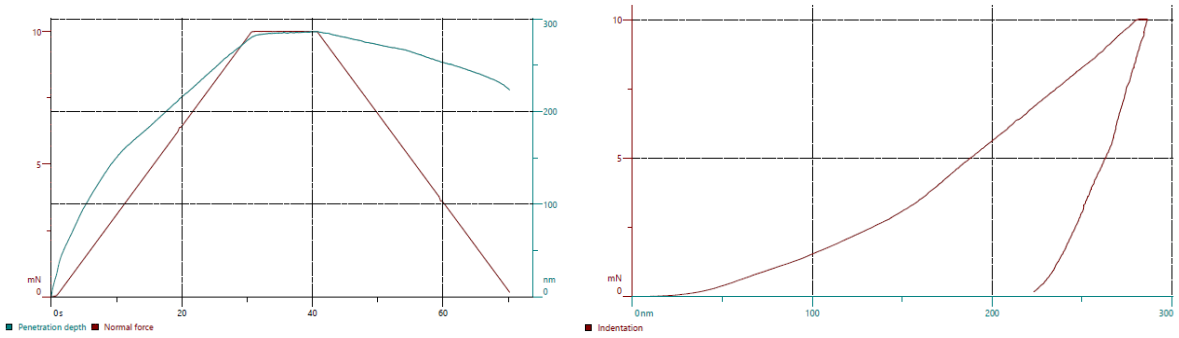
The nanoindentation results revealed noticeable differences in the mechanical properties of the investigated HEA coatings, indicating a significant influence of the deposition parameters on coating formation and microstructural development. The measured indentation hardness (HIT), which represents the material's resistance to localized plastic deformation under an applied load, ranged approximately between 7 and 9 GPa for the coated samples. In all cases, the HEA coatings exhibited higher hardness values than the uncoated substrate, confirming the successful formation of mechanically strengthened surface layers. In addition to HIT, the Vickers indentation hardness (HVIT) was determined from the nanoindentation data.

Table 5. *Nanoindentation measurement results*

	HIT [GPa]	HVIT	E* [GPa]
1	7,74	696	205
2	7,52	694	211
3	7,84	806	226
4	7,75	694	222
5	8,32	744	210
6	7,51	694	213
7	8,81	837	270
8	7,07	705	247
9	8,01	811	249
SS316	5,73	545	220

Although derived from instrumented indentation measurements, HVIT provides a more familiar hardness scale and followed trends similar to those observed for HIT. The obtained results indicate

that variations in sputtering parameters led to measurable changes in coating hardness, suggesting differences in coating density, grain structure, and phase composition.
The reduced elastic modulus (E*) was also evaluated as an indicator of the elastic response of the coating-substrate system. Higher E* values generally correspond to increased stiffness and greater resistance to elastic deformation under contact loading. The measured values were within the typical range reported for magnetron-sputtered HEA coatings and demonstrated that the deposited layers possessed not only high hardness but also sufficient mechanical rigidity.
The reduced elastic modulus values generally ranged from approximately 200 to 270 GPa for most coated samples, indicating relatively consistent elastic behaviour among the deposited coatings. The sample 7 exhibited the highest scatter in mechanical properties, which may be associated with local microstructural inhomogeneity or measurement variability. Overall, the obtained results confirm the improved mechanical performance of the HEA-coated surfaces compared to the uncoated substrate.



a) b)

Figure 8. *Nanoindentation curve for Sample 3 a) Penetration depth, b) Indentation force*

4. Conclusion

FeCrCoMnNi high-entropy alloy coatings were successfully deposited on stainless steel substrates by DC magnetron sputtering using a WAAM-fabricated HEA target. The obtained results demonstrated that variations in sputtering parameters significantly influenced both the tribological and mechanical properties of the coatings. Nanoindentation measurements confirmed an increase in hardness compared to the uncoated substrate, while tribological testing revealed distinct differences in friction behaviour among the investigated samples under various sliding conditions. Among the tested coatings, Sample 4 exhibited the most favourable tribological response under severe loading conditions. Overall, the results demonstrate that WAAM-fabricated FeCrCoMnNi targets can be successfully utilized for the deposition of HEA coatings by magnetron sputtering and represent a promising approach for the development of protective coatings with tailored tribological and mechanical properties.

Acknowledgments

This work was supported by the European Union under the NextGenerationEU instrument, through the Recovery and Resilience Mechanism, within the institutional research project AIMTECH 4.5 (IP-UNIST-07), implemented by the Ministry of Science, Education and Youth of the Republic of Croatia.
The authors thank AntonPaar Croatia d.o.o. for providing technical support and loaning the TRB3 and HIT3 equipment used to collect the tribological and nanoindentation data presented in this study.

References

[1] W. Zhang, P. K. Liaw, and Y. Zhang, ‘Science and technology in high-entropy alloys’, *Sci. China Mater.*, vol. 61, no. 1, pp. 2–22, Jan. 2018, doi: 10.1007/s40843-017-9195-8.
[2] L. Han *et al.*, ‘Multifunctional high-entropy materials’, *Nat Rev Mater*, vol. 9, no. 12, pp. 846–865, Sep. 2024, doi: 10.1038/s41578-024-00720-y.

[3] S. El-Hadad, ‘High Entropy Alloys: The Materials of Future’, *International Journal of Materials Technology and Innovation*, vol. 2, no. 1, pp. 67–84, Apr. 2022, doi: 10.21608/ijmti.2022.118565.1046.
[4] C. Sha, Z. Zhou, Z. Xie, and P. Munroe, ‘High entropy alloy FeMnNiCoCr coatings: Enhanced hardness and damage-tolerance through a dual-phase structure and nanotwins’, *Surface and Coatings Technology*, vol. 385, p. 125435, Mar. 2020, doi: 10.1016/j.surfcoat.2020.125435.
[5] N. NayebPashaee *et al.*, ‘High-entropy alloy coatings for surface protection and thermal barrier applications: fundamentals, recent advances, and a critical assessment of their potential as alternatives to conventional coatings’, *Discov Mater*, vol. 6, no. 1, p. 11, Dec. 2025, doi: 10.1007/s43939-025-00480-8.
[6] S. K. Padamata, A. Yasinskiy, V. Yanov, and G. Saevarsdottir, ‘Magnetron Sputtering High-Entropy Alloy Coatings: A Mini-Review’, *Metals*, vol. 12, no. 2, p. 319, Feb. 2022, doi: 10.3390/met12020319.
[7] Y. S. Kim, H. J. Park, K. S. Lim, S. H. Hong, and K. B. Kim, ‘Structural and Mechanical Properties of AlCoCrNi High Entropy Nitride Films: Influence of Process Pressure’, *Coatings*, vol. 10, no. 1, p. 10, Dec. 2019, doi: 10.3390/coatings10010010.
[8] Q. Zeng and Y. Xu, ‘A comparative study on the tribocorrosion behaviors of AlFeCrNiMo high entropy alloy coatings and 304 stainless steel’, *Materials Today Communications*, vol. 24, p. 101261, Sep. 2020, doi: 10.1016/j.mtcomm.2020.101261.
[9] Y.-S. Kim, H.-J. Park, J.-O. Seo, J.-W. Shin, S.-H. Hong, and K.-B. Kim, ‘Studies on the Morphological and Mechanical Properties of TiZrHfNiCuCo Metallic Coatings Deposited by DC Magnetron Sputtering’, *Coatings*, vol. 14, no. 9, p. 1179, Sep. 2024, doi: 10.3390/coatings14091179.
[10] A. Sobetkii *et al.*, ‘Deposition and Characterization of Cu-Enhanced High-Entropy Alloy Coatings via DC Magnetron Sputtering’, *Applied Sciences*, vol. 15, no. 4, p. 1917, Feb. 2025, doi: 10.3390/app15041917.
[11] J. Wang, S. Kuang, X. Yu, L. Wang, and W. Huang, ‘Tribo-mechanical properties of CrNbTiMoZr high-entropy alloy film synthesized by direct current magnetron sputtering’, *Surface and Coatings Technology*, vol. 403, p. 126374, Dec. 2020, doi: 10.1016/j.surfcoat.2020.126374.
[12] Q. S. Chen *et al.*, ‘Microstructure and corrosion characteristics of CrCuFeMoNi HEA coatings with different compositions in high-temperature and high-pressure water’, *Mater. Res. Express*, vol. 6, no. 8, p. 086511, May 2019, doi: 10.1088/2053-1591/ab19ed.
[13] M. El Garah, D. Soubane, and F. Sanchette, ‘Review on mechanical and functional properties of refractory high-entropy alloy films by magnetron sputtering’, *emergent mater.*, vol. 7, no. 1, pp. 77–101, Feb. 2024, doi: 10.1007/s42247-023-00607-8.
[14] C. Huang *et al.*, ‘Magnetron-sputtered high-entropy coatings: Plasma control, microstructure, and tribological performance’, *Surface and Coatings Technology*, vol. 525, p. 133283, Apr. 2026, doi: 10.1016/j.surfcoat.2026.133283.
[15] Y. X. Ye, C. Z. Liu, H. Wang, and T. G. Nieh, ‘Friction and wear behavior of a single-phase equiatomic TiZrHfNb high-entropy alloy studied using a nanoscratch technique’, *Acta Materialia*, vol. 147, pp. 78–89, Apr. 2018, doi: 10.1016/j.actamat.2018.01.014.
[16] C. Zhang *et al.*, ‘Tailoring the microstructure, mechanical and tribocorrosion performance of (CrNbTiAlV)N high-entropy nitride films by controlling nitrogen flow’, *Journal of Materials Science & Technology*, vol. 107, pp. 172–182, Apr. 2022, doi: 10.1016/j.jmst.2021.08.032.
[17] N. Behravan, A. Farhadizadeh, S. Ghasemi, A. Khademi, H. Shojaei, and H. Ghomi, ‘The pressure dependence of structure and composition of sputtered AlCrSiTiMoO high entropy thin film’, *Journal of Alloys and Compounds*, vol. 852, p. 156421, Jan. 2021, doi: 10.1016/j.jallcom.2020.156421.
[18] Ph. V. Kiryukhantsev-Korneev, A. D. Chertova, F. I. Chudarin, E. I. Patsera, and E. A. Levashov, ‘The structure and properties of high-entropy (MoTaNbZrHf)-Si-B coatings deposited by DCMS and HIPIMS methods using the multilayer target’, *Surface and Coatings Technology*, vol. 484, p. 130797, May 2024, doi: 10.1016/j.surfcoat.2024.130797.

[19] Y. Wang *et al.*, ‘Microstructure and tribological performance of (AlCrWTiMo)N film controlled by substrate temperature’, *Applied Surface Science*, vol. 574, p. 151677, Feb. 2022, doi: 10.1016/j.apsusc.2021.151677.

[20] J. Krolo, A. Nagode, M. Kljajo, N. Čatipović, I. Peko, and D. Jurić, ‘Tribological and microstructural characterization of thermal-sprayed Cr-Ni- Mo coatings on stainless steel’, presented at the International conference “Mechanical Technologies and Structural Materials”, MTSM 2025, Split, 2025, pp. 177–188.

[21] M. Khadem, O. V. Penkov, H.-K. Yang, and D.-E. Kim, ‘Tribology of multilayer coatings for wear reduction: A review’, *Friction*, vol. 5, no. 3, pp. 248–262, Sep. 2017, doi: 10.1007/s40544-017-0181-7.